

In-flight performances of the PAMELA magnetic spectrometer

**O. Adriani,^{a,b} M. Bongi,^{a,b} L. Bonechi,^{a,b} S. Bottai,^a G. Castellini,^{a,c} D. Fedele,^{a,b}
M. Grandi,^a G. Landi,^{a,b} P. Papini,^a S. Ricciarini,^a P. Tasselli,^{a,b} E. Taddei,^{a,b}
E. Vannuccini^{*a}**

^a*INFN, Structure of Florence, Via Sansone 1, I-50019 Sesto Fiorentino, Florence, Italy*

^b*Physics Department of the University of Florence, Via Sansone 1, I-50019 Sesto Fiorentino, Florence, Italy*

^c*IFAC, Via Madonna del Piano 10, I-50019 Sesto Fiorentino, Florence, Italy*

E-mail: vannuccini@fi.infn.it

PAMELA is a satellite-borne experiment designed to study charged particles in the cosmic radiation with a particular interest in antiparticles. The experiment is collecting data since July 2006 on board of the Russian Resurs DK1 satellite, which travels along a semipolar elliptical orbit around the Earth. The PAMELA apparatus includes a magnetic spectrometer, which is composed of 6 planes of silicon microstrip detectors dipped in an almost-uniform magnetic field generated by a permanent magnet made of Nd-Fe-B alloy. The spectrometer has been designed to determine precisely the rigidity (up to 1 TeV) and the absolute charge (up to $Z=6$) of particles crossing the detector.

In the first part a short review of the magnetic spectrometer design is given and the main spectrometer operations in flight are described. The main topic of this article is the procedure to measure the rigidity, described in the second part. Particular focus is put on the position-finding algorithm. In fact, recent theoretical and experimental results have shown that in case of inclined tracks a significant systematic shift can be present, if the proper algorithm is not applied. Finally, some preliminary results are presented.

*16th International Workshop on Vertex detectors
September 23-28 2007
Lake Placid, NY, USA*

*Speaker.

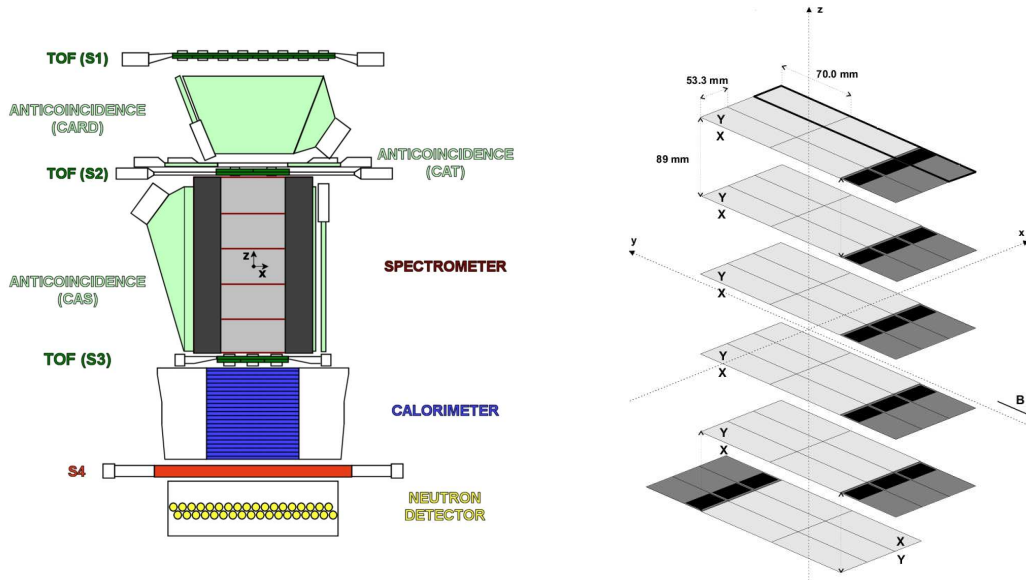


Figure 1: Left: schematic view of the PAMELA apparatus. Right: schematic view of the tracking-system planes. The PAMELA reference system and the main direction of the magnetic field are also shown.

1. Introduction: the PAMELA experiment

PAMELA [1] is a satellite-borne experiment that has been designed to study light charged particles in the cosmic radiation, with a particular focus on antiparticles (\bar{p} and e^+). PAMELA is installed on board the Russian Resurs-DK1 Earth-observation satellite that has been launched into space with a Soyuz-U rocket on June 15th, 2006 from the Baikonur cosmodrome in Kazakhstan.

The primary scientific goal of the experiment is to extend the experimental knowledge about the antimatter component in cosmic rays over an energy range (80 MeV \div 190 GeV for \bar{p} and 50 MeV \div 270 GeV for e^+) wider than covered so far, mainly by balloon-borne experiments; moreover, the long duration of the mission, foreseen to last at least 3 years, will allow to collect an unprecedented statistics.

A schematic overview of PAMELA is shown in fig. 1 (left). The core of the apparatus is the silicon-microstrip magnetic spectrometer, which mainly provides a measurement of the magnetic rigidity ($R = pc/Ze$) and the sign of the electric charge. The latter quantity is a basic information in order to separate \bar{p} from p and e^+ from e^- . A silicon-tungsten electromagnetic calorimeter, complemented at high energy by the shower-tail catcher (S4) and the neutron detector, provides the required electron/hadron (e^+/p and \bar{p}/e^-) separation above $\sim 1GV$. At low energy particle identification is accomplished mainly by means of the β information provided by the time-of-light system (TOF); this also allows to reject albedo¹ protons, which as seen by the spectrometer would mimic \bar{p} . An anticounter system (CARD, CAT and CAS) surrounds the magnetic spectrometer and the gap between the top and the middle TOF planes. Its information is used offline to tag events where there are particles outside the instrument acceptance, which might indicate that an interaction occurred in the surrounding material and the trigger was given by secondaries; in these

¹ Cosmic-ray particles that enters the apparatus from below.

cases a single π^- produced in the interaction could enter the spectrometer and be identified as an \bar{p} . Multiple (dE/dx) measurements, from the spectrometer silicon planes, the TOF scintillators and the first plane of the calorimeter allow charge identification.

The magnetic spectrometer has a key role in the antiproton measurement at high energy. In fact, the upper limit in the antiproton energy is set by the *spillover*-proton background, which comes from the wrong determination of the charge sign due to the finite resolution of the instrument. This source of background is most important for high-energy antiprotons because of the large amount of protons present in cosmic rays ($\bar{p}/p \sim 10^{-4}$). Thus, optimal performances of the spectrometer are of major importance for the PAMELA science.

2. Magnetic spectrometer design

PAMELA scientific objectives require an extremely good momentum resolution. This can be achieved by having a micrometric spatial resolution and a reduced amount of material traversed by the particle into the tracking volume. The natural choice has been to use microstrip silicon detectors, which satisfy both the requirements. Besides science requirements, the design had also to comply with several constraints imposed by the satellite mission (eg. limitations in mass and power consumption, etc.). A detailed description of the instrument, as well as the main developments in the design during the years, can be found in reference [2] and references therein. Here we give few details, useful to better understand the arguments of the following sections.

The spectrometer is composed of a permanent magnet, with a central rectangular cavity of $16.14 \times 13.14 \times 43.66$ cm³, and a tracking system, with 6 equidistant planes of silicon detectors inserted inside the magnet cavity. The magnet is a tower of 5 identical modules made of Nd-Fe-B blocks assembled in an aluminum mechanics and arranged so that they provide a magnetic field mainly directed along the y axis (see fig. 1, right). In order to guarantee a good track reconstruction, the field components, inside and outside the magnet cavity, have been measured over a spatial grid of 5 mm pitch. The field intensity is ~ 0.48 T at the center of the magnet. Each plane of the tracking system (see fig. 1) has 3 independent sections (*ladders*), each composed of 2 double-sided n-type silicon sensors, 5.33×7.00 cm² wide and 300 μ m thick, and a hybrid circuit. The implant pitch is 25.5 μ m on the junction side (2035 strips) and 66.5 μ m on the ohmic side (1024 strips). Strips on opposite sides are orthogonal. On the junction side only one out of two strips is readout. On both sides charge readout is done through an integrated capacitive coupling obtained by means of a thin layer of SiO₂ between implanted and readout strips. On the ohmic side a second metal layer, with metallic strips orthogonal to the ones below, bring the electric signals on the same edge of the sensor, which is connected with the hybrid circuit. The junction side, which has better performances, is used to measure the coordinate along the bending direction (x axis fig. 1).

The hybrid circuit houses the front-end electronics, which is based on 288 VA1 chips [3]. The operating point of the chip, characterized by very low-noise and low-power consumption, has been set for an optimal compromise between a reduced dissipation (37 W for 36864 channels) and a good S/N ratio, with a dynamic range up to ~ 10 MIP.

The subsequent readout stages, placed outside the magnetic tower, include 36 12-bit ADCs and 12 DSPs that perform online data compression and calibration. Data compression, which is necessary due to the limited bandwidth for data transfer to ground, is achieved by means of a zero-

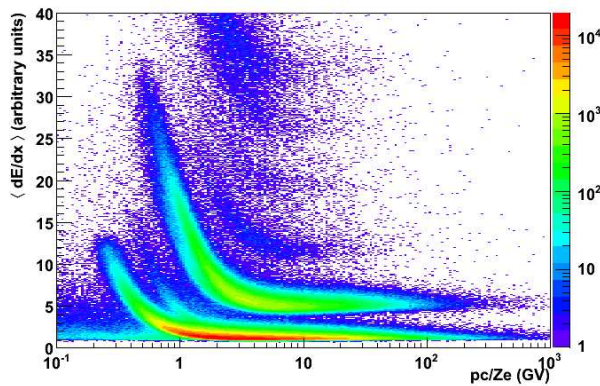


Figure 2: Average dE/dx as a function of the measured rigidity for a sample of positively charged particles selected from flight data.

order predictor algorithm, modified in order to fully transmit particle signals. Ground test of the detectors have shown that a compression factor of ~ 20 can be achieved without losing significant information. This is essential to obtain optimal performances in the impact-point reconstruction.

3. In-flight operations and basic performances

All the operations are handled automatically by the main CPU, which controls the flow of PAMELA physics tasks and continuously checks the status of the apparatus [4].

The Resurs-DK1 travels along a semi-polar orbit in about 95 min, at an height varying between 350 and 600 km and with an inclination of about 70° . The acquisition rate varies along the orbit as a function of the geomagnetic location and is on average 25 Hz. The amount of data collected is about ~ 5 kB/event. In spite of the strong compression applied, most of the data comes from the spectrometer, which collect ~ 3 kB/event. The compressed output is checked event-by-event in order to detect possible anomalies (eg. latch-up, compression inefficiency, etc.). In case of anomalous conditions an alarm line is asserted and an action can be taken by the CPU (reset or power off/on).

All detectors are calibrated almost once per orbit, when the satellite crosses the equator from the southern to the northern hemisphere, which is the point of lowest particle rate. During the spectrometer calibration the complete map of pedestals, noises (after common-noise subtraction) and bad channels is evaluated and stored to be used in the following acquisition runs, in order to improve data compression. The calibration output is checked online by the CPU and repeated if anomalous values are found; in case of any failure during the calibration procedure, default maps are loaded until the next successful calibration.

The thermal environment is fundamental to guarantee stability of operation for the magnetic spectrometer. Several temperature sensors are placed on the external walls of the magnetic tower: the registered temperatures increase from $\sim 21^\circ\text{C}$, when the system is off, to $\sim 31^\circ\text{C}$, when the system is on, with variations of less than 1°C at regime.

PAMELA can be remotely controlled through commands sent from ground, which, among other actions, allow to configure the system by setting proper parameters. Both the spectrometer acquisition and calibration procedures have been implemented with many modifiable parameters (eg. compression parameters, thresholds for the calibration check, etc.), so that the system can be

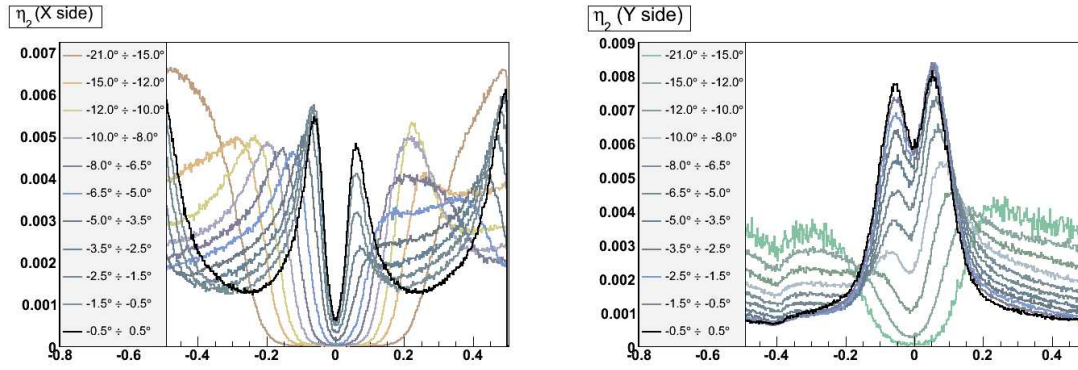


Figure 3: Distribution of the η_2 variable, $H(\eta_2)$, as a function of the track projected angle, relative to the sensor, for the x (left) and y (right) sides.

easily adapted to space (partially unknown) conditions. A quick semi-automatic check of the data is performed each time data are transferred to ground (about twice per day). In case of anomalies, or simply for test purpose, commands can be sent to PAMELA in few hours.

A more refined check of the basic instrument performances is done offline, by studying particle signals. The charge deposited by a particle is usually collected by few strips (*clusters*). The cluster S/N ratio² observed in flight [2] is consistent with the value measured on ground (~ 56 and ~ 26 , for the x and y sides respectively) indicating the good performances of the instrument. Fig. 2 shows the average dE/dx measured by the tracker as a function of the rigidity, obtained for a sample of positively charged particles selected from flight data. The good separation among different charge families is evident from the plot. Furthermore, at low energy also H and He isotopes can be distinguished. Above Be charge separation is affected by the single-channel saturation, as expected from the dynamic range of the spectrometer silicon detectors measured at beam tests (^{12}C -beam test of ladder prototypes, GSI, 2006 [5]).

4. Position reconstruction

Position reconstruction in silicon microstrip detectors is a key point to reach the optimal performances of the system; in order to achieve the micrometric resolution typical of these sensors the cluster signal has to be treated with proper algorithms. In addition, the absolute positions of the tracking-system sensors have to be known with the proper accuracy. These aspects are separately discussed in the next sections.

4.1 Position-finding algorithm

In order to discuss about position-finding algorithms it is useful to introduce the variable:

$$\eta_n = \frac{\sum_n p s}{\sum_n s} \quad (4.1)$$

where p is the strip coordinate relative to the strip with the maximum signal, expressed in pitch units, s is the strip signal and the sum is over $n = 1, 2, \dots$ strips around the cluster. The hit coordinate

²Defined here as the sum of the S/N ratio of all the strips belonging to the cluster.

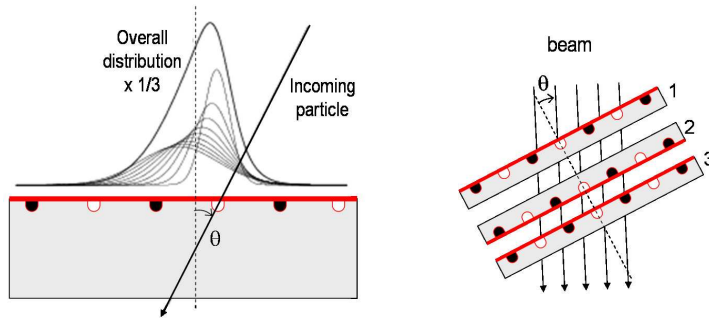


Figure 4: Left: schematic drawing of the signal distribution generated by inclined tracks. Right: schematic view of the beam-test setup.

relative to the sensor can be derived from the general expression:

$$x = P \cdot f(\eta_n) + x_{max} \quad (4.2)$$

where P is the strip pitch, x_{max} is the coordinate of the strip with the maximum signal and f is a non-decreasing function of the variable η_n . The most simple way to evaluate the coordinate is the cluster *center of gravity*, which is obtained by replacing $f(\eta_n) = f_n$ in eq. 4.2; in fact, η_n is by definition the cluster center of gravity, relative to the strip with the maximum signal, expressed in pitch units.

However, as is well known, the center-of-gravity is not the best estimator of the impact coordinate; in fact, due to discretization effect of the signal distribution, charge sharing among adjacent strips in silicon microstrip sensors is not linear. This feature is evident in fig. 3, which shows the distribution $H(\eta_2)$ of the variable η_2 , obtained from flight data, as a function of the track projected-angle relative to the sensor, for the x and y views, respectively. At small angles most of the charge is collected by 2 strips³. Thus, in principle, a 2-strip center of gravity could be used to evaluate the coordinate; but if η_2 was a good coordinate estimator, the distributions in fig. 3 would be flat.

When charge collection is not linear, the best estimate of the impact coordinate is given by the η_2 -algorithm. According to this method, the impact coordinate is evaluated as the integral of the experimental η_2 -distribution, $H(\eta_2)$:

$$f(\eta_2) = f(\eta_0) + \int_{\eta_0}^{\eta_2} H(h) dh. \quad (4.3)$$

In a standard implementation of the algorithm, $f_s(\eta_2)$, the integral starts at $\eta_0 = -0.5$ and the integration constant is $f_s(-0.5) = -0.5$. The spatial resolution obtained by applying this algorithm has been studied during the past years by means of beam-test data and simulation [7]. In particular, the evaluated resolution on the x side, which is used to measure the coordinates along the bending direction, is $\sim 3\mu\text{m}$ up to 5° ; above 10° , simulation shows that better results are obtained by using more than 2 strips in the evaluation of the impact coordinate, since the deposited charge is collected by more strips. In this case eq. 4.3 can be generalized to η_3 , η_4 , etc. On the y view, where the pitch is larger, a 2-strip algorithm gives the best result up to 20° .

In spite of the good resolution achieved with the η_2 -algorithm, one should notice that the choice of the integration constant in eq. 4.3 relies on the assumption of a symmetric signal distribution. In fact, only in this case one can assume that if the charge is equally shared between 2

³Since in this article mostly results at small angles are shown, in the following we restrict the discussion to 2-strip algorithms.

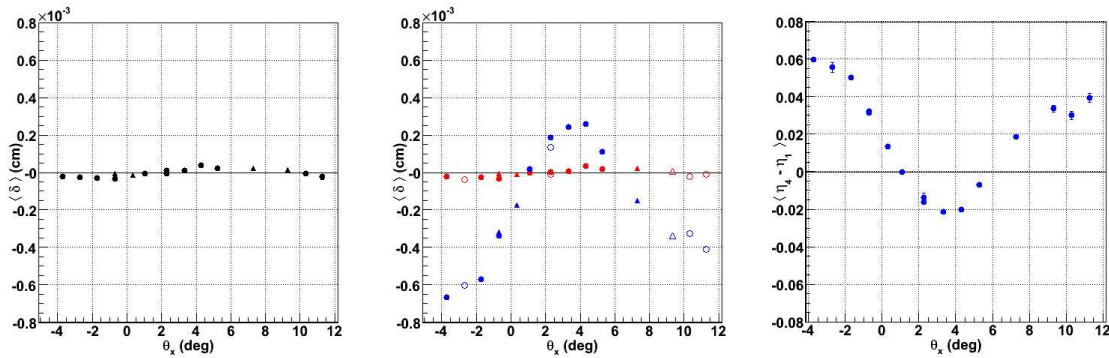


Figure 5: Left: measured spatial residuals as a function of the track angle obtained with 4-strip center of gravity. Center: same as left plot, but obtained with standard η_2 -algorithm (blue markers) and corrected η_2 -algorithm (red markers). Right: angular correction Δ , expressed in pitch units. Results are from beam-test data (CERN-SPS, 2006).

strips ($\eta_2 = \pm 0.5$) the particle impact coordinate is exactly $f_s(\pm 0.5) = \pm 0.5$. The consequence is that any asymmetry in the signal distribution introduces a systematic shift of the coordinate, if the standard η_2 -algorithm is applied. From eq. 4.3:

$$f(\eta_2) = f_s(\eta_2) + \Delta \quad (4.4)$$

where f_s is the coordinate obtained with the standard η_2 -algorithm and $\Delta = f_s(-0.5) + 0.5$ is a correction to be applied in order to cancel out the shift. The symmetry condition is not satisfied in case of inclined tracks, as it is illustrated in fig. 4.1 (left).

The angular effect on the position reconstruction with silicon microstrip detectors has been extensively studied by Landi [8, 9] by means of both an analytical model, based on signal theory, and statistical simulations. More generally, the author studied the effect of discretization of the signal distribution, due to the detector segmentation, on the evaluation of the coordinate. Both the analytical model and the simulation have been tuned on PAMELA tracker sensors. From an experimental point of view, the main results of this study are the following: (1) the standard η_2 -algorithm gives a significant systematic coordinate-shift on the x side ($\sim 2\mu\text{m}$ at 3°); (2) the center of gravity evaluated with 4 strips (or more), η_4 , gives no shifts (but worse resolution); (3) the correction can be derived from data itself as:

$$\Delta \sim \langle \eta_4 \rangle \quad (4.5)$$

where the average is evaluated over all the clusters at a fixed angle.

In order to measure the angular effect, a dedicated beam test was performed in 2006 with protons of momentum $50 \div 150$ GeV/c, at the CERN-SPS facility. For this purpose, a small tracking system made of five planes was prepared. Prototypes of the tracking-system ladders were used, having the same silicon sensors, front-end electronics and readout system. In this case no data compression was applied. The detector was placed on a turntable, so that the beam angle relative to the x side of the sensors could be varied. Three of the five planes were placed at a closer distance, in order to minimize multiple scattering effect on the measured coordinates, and the middle plane was rotated of 180° around the y axis (see fig. 4.1, right); with this setup the spatial residual on the

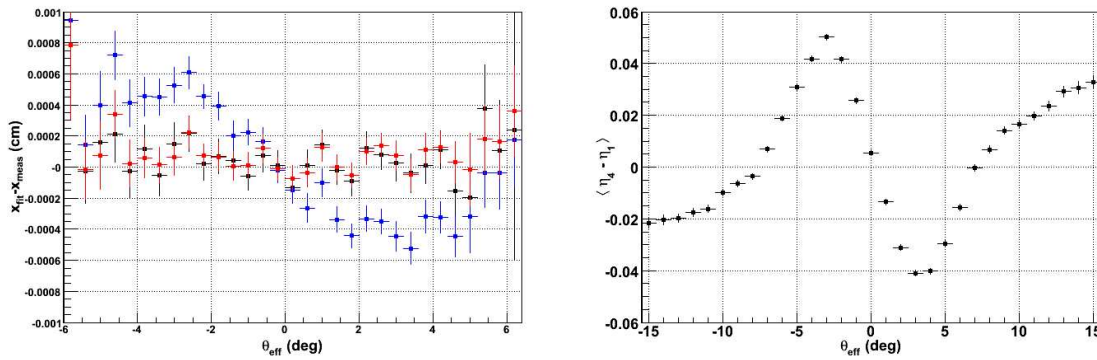


Figure 6: Left: mean value of the measured spatial residual on the x view of the bottom plane, obtained with the 4-strip center of gravity (black markers). Points indicated by triangles (samples at 0° , 7° and 9°) refer to the data used to align the system. Center: residuals obtained by applying the standard η_2 -algorithm (blue markers) and the corrected η_2 -algorithm (red markers). Right: angular correction Δ , expressed in pitch units. Results are from flight data.

x side of the middle plane, evaluated as $\delta = x_2 - (x_1 + x_3)/2$, is equal to twice the coordinate shift, if any.

The left plot in fig. 5 shows the average spatial residual δ as a function of the angle, obtained by evaluating the coordinate with the 4-strip center of gravity. The mean value of the residuals indicates that the 4-strip center of gravity is not affected by significant angular systematics, within $1\mu\text{m}$. The blue markers on the second plot of fig. 5 show the average spatial residuals obtained by applying the standard η_2 -algorithm; a systematic shift is evident in this case, which is maximum at $\sim -4^\circ$. The red markers show the residuals after the angular correction Δ , evaluated from eq. 4.5, has been applied: the correction, shown on the rightmost plot, bring the systematic shift to the level of less than $1\mu\text{m}$, which is consistent with what is obtained by applying the 4-strip center of gravity. An unexpected feature in fig. 5 is that the coordinate shift is different from zero at 0° , where a symmetric signal distribution would be expected. The cause of this asymmetry is currently under investigation; however, whatever the reason is, the correction accounts for it.

The angular effect on the reconstructed coordinate could also be put in evidence on flight data. In fact, as shown in fig. 1, the bottom plane of the tracking system is rotated of 180° around the x axis: the consequence is that on this plane the shift of the reconstructed x coordinate has opposite sign, in comparison with the other planes. In order to check the angular effect, a sample of relativistic protons with 6 hits on both the x and y views have been selected: the bottom plane has been removed from the track fitting, since the shift would have biased the fit result, and the spatial residual on x view has been calculated. The results, for different position-finding algorithms, are shown in fig. 6 (left plot), where the mean value of the residual is plotted as a function of the angle. Again, a significant shift can be noticed if the standard η_2 -algorithm is applied (blue markers), which is corrected by adding Δ (right plot in fig. 6) to the reconstructed coordinate. By comparing fig. 6 (right) and fig. 5 (right) one can notice that the asymmetry is less evident in the case of flight data.

Fig. 7 shows the residual distribution on the bottom plane obtained from flight data, for the three different position-finding algorithms (left plot) and compared with simulation (right plot).

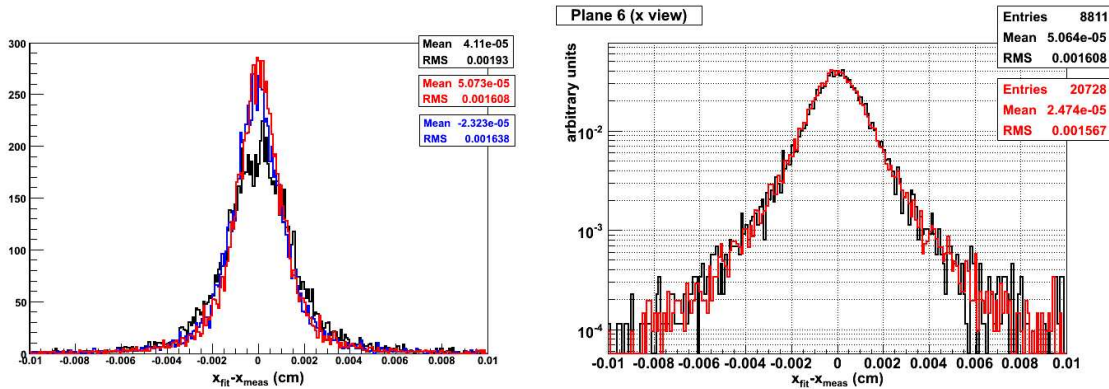


Figure 7: Left: distribution of the measured spatial residual on the x view of the bottom plane, obtained with the 4-strip center of gravity (black line), the standard η_2 -algorithm (blue line) and the corrected η_2 -algorithm (red line). Results are from flight data. Right: comparison between flight data (black line) and simulation (red line), for the corrected η_2 -algorithm.

As expected, the corrected η_2 -algorithm gives the best resolution. The good agreement with the simulation indicates that the detector tracking performances are well understood.

4.2 Sensor alignment

In order to profit of the excellent spatial resolution of the detectors, the absolute positions of the silicon sensors in the general PAMELA reference frame have to be known with an uncertainty less than $\sim 1 \mu\text{m}$. Mechanical processing does not guarantee the required precision, thus a software alignment has been necessary. The only possibility for the PAMELA spectrometer is a track-based alignment, which consists in minimizing the spatial residuals as a function of the roto-traslation parameters of the sensors. A complication with this approach is that tracks are bent by the magnetic field generated by the permanent magnet; thus the curvature of the particle trajectory has to be known a priori and this requires an independent estimate of the particle rigidity.

The tracking system has been first aligned at ground with a 100 GeV/c proton beam (beam-test of the spectrometer flight-model, CERN-SPS, 2003) and the alignment has been cross-checked with atmospheric muons (PAMELA integration, INFN laboratory, 2005), by studying the muon charge-ratio; the evaluated corrections to the nominal position of the sensors were $\sim 100 \mu\text{m}$.

In flight further corrections are required, in order to account for sensor movements occurring mainly during the launch phase. Since the linear dilatation coefficient of silicon sensor is $\sim 2.6 \text{ }^\circ\text{C}^{-1}$, sensor dilatation due to temperature variations can be neglected. This second-order alignment has been done with relativistic protons; since no independent energy measurement is available in this case, the alignment is done by fixing the deflection at the measured value. This procedure allows to correct for the relative displacements among sensors (the estimated corrections amounts to $\sim 10 \mu\text{m}$), but might results in an overall distortion of the reconstructed tracks. Global distortions of the system can mimic a curvature, thus resulting in a systematic error on the reconstructed deflection. The possibility to check the spectrometer systematics is provided by electrons and positrons, whose energy can be measured with the calorimeter. This work is still in progress.

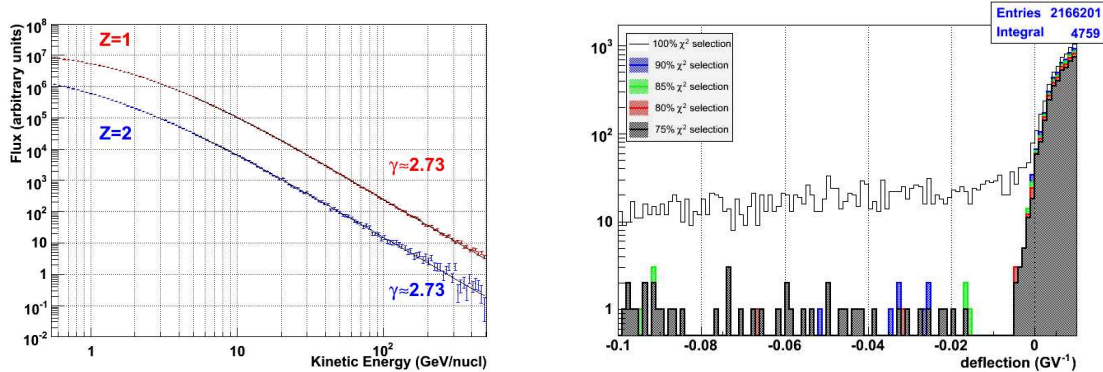


Figure 8: Preliminary results from flight data. Left: H and He spectra. Right: distribution of measured deflection for a sample of singly charged particles, after electrons have been rejected, as a function of the χ^2 selection efficiency. The antiproton component, on the left, is well separated from the proton spillover background.

5. Momentum measurement

First step in order to measure the particle momentum is to associate the measured points to a physical track. Track recognition is not a main issue, since for the purpose of the experiment good events are clean single tracks going through the apparatus. A combinatorial implementation of the Hough transform is applied, independently, to the x and y projections; at this stage the trajectory is approximated with a circle arc and a straight line, respectively. Preliminary studies indicate that the track identification efficiency for singly charged particles is close to what expected from detector geometry.

Track fitting is based on a χ^2 minimization of the spatial residuals as function of the track parameters: $\alpha = (x_0, y_0, \cos \theta, \phi, d)$, where the first four components express the trajectory intersection-point and direction on a reference plane $z_0 = \cos \theta$ and d is the magnetic deflection, defined as the inverse of the rigidity: $d = 1/R$. An iterative analytical method [10] is applied in order to find the track state-vector α that minimize the χ^2 . The particle trajectory is evaluated with a stepwise numerical integration of motion equations in the non-homogeneous magnetic field. The three components of the magnetic field are calculated in each point by means of a 3-dimensional interpolation of the measured field map.

At high energy, where multiple scattering is negligible, the spectrometer measurement is affected by a constant deflection error Δd , which is directly related to the position error. The performances of spectrometers designed for cosmic-ray studies are usually expressed through the *maximum-detectable-rigidity* parameter (*MDR*), which is defined as the value of the rigidity that is affected by an error of 100%: by definition, $\Delta R/R = R/MDR$ where $MDR = 1/\Delta d$. The momentum resolution has been measured with proton beams and results of the analysis have demonstrated that an *MDR* of ~ 1 TV can be achieved [1]. This result is also confirmed by simulation.

6. Preliminary results

Even if at an early stage of the detector calibration, the results discussed above indicate that the

spectrometer is behaving nominally and a reliable estimate of the particle rigidity can be expected. As a further confirmation of this statement, it is useful to show some results on the measured-energy distributions of cosmic rays.

Fig. 6 (left) shows the H and He galactic spectra, obtained from a sample of events corresponding to about 100 days of acquisition; $Z=1$ and $Z=2$ particles have been selected by means of a dE/dx vs rigidity cut (fig. 2) and the spectra have been corrected for the geomagnetic transmission factor. No efficiency correction has been applied. The shape of the spectra is consistent with an high-energy spectral index $\gamma \sim 2.73$, which is an average value deduced from previous measurements.

As discussed in section 1, the most difficult task of the spectrometer is the rejection of proton-spillover background from the antiproton sample. Antiprotons are identified by selecting singly charged particles and by rejecting both electrons (by means of the calorimeter information) and albedo protons (by means of the time-of-light system). The best performances for a magnetic spectrometer are obtained by maximizing the track length; thus, one good hit (no bad channels) on the top and the bottom planes has been required on the bending view. The deflection distribution resulting after the selections is shown in the right plot of fig. 6, for a small sample of flight data (~ 100 days). The antiproton component is clearly visible on the left side of the plot (negative deflection); for increasing deflection, while approaching $d = 0$, the spillover protons start to contaminate the sample. The amount of spillover protons is strongly related to the deflection error; in order to reach the highest energy in the antiproton selection, strong requirements must be applied to the quality of the track. For this purpose, the most effective cut is that on the χ^2 , whose effect is shown fig. 6 (right) by different colors; the variation in the number of candidate antiprotons is consistent with the χ^2 -selection efficiency estimated for protons (top-left text box inside the picture).

7. Conclusion

The PAMELA experiment is collecting data almost continuously since July 2006 and individual detector calibrations are currently under progress. Among the detectors, the magnetic spectrometer plays a crucial role for the experiment, since it provides the main particle-energy measurement.

Much effort is being put in improving the hit coordinate evaluation: the angular effect on the position determination has been studied and corrections to the standard position-finding-algorithm have been applied. Comparison between flight data and simulation indicates that the spatial performances of the detector are nominal. A preliminary analysis of the flight data confirms that the spectrometer is providing a reliable estimate of the rigidity over a wide energy range. In particular, the spillover background is under control and the energy upper limit for antimatter search is close to the design value.

References

- [1] P. Picozza et al., *PAMELA - A Payload for Antimatter Matter Exploration and Light-nuclei Astrophysics*, *Astropart.Phys.* **27** (296) 2007 [astro-ph/0608697]
- [2] S. Ricciarini et al., *PAMELA Silicon tracking system: experience and operation*, Proceedings of *VERTEX 2006*

- [3] <http://www.ideas.no>
- [4] P. Picozza et al., *PAMELA: an Experiment for Antiparticles Measurement in Cosmic Rays*, Proceedings of *XII International Workshop on Neutrino Telescopes 2007*; E. Vannuccini et al., *In-flight status of the PAMELA experiment*, Proceedings of *International Workshop on Cosmic Rays and High-energy Universe 2007*
- [5] R. Sparvoli et al., *Capability of the PAMELA instrument to identify light-nuclei: results from a beam test calibration*, Proceedings of *20th ECRS 2006*
- [6] R. Turchetta et al., *Spatial resolution of silicon microstrip detectors*, *Nucl.Instrum.Meth A* **335** (44) 1993
- [7] S. Straulino et al., *Spatial resolution of double-sided silicon microstrip detectors for the PAMELA apparatus*, *Nucl.Instrum.Meth A* **556** (100) 2006 [hep-ex/0510012]
- [8] G. Landi, *Properties of the center of gravity as an algorithm for position measurements*, *Nucl.Instrum.Meth A* **485** (698) 2002
- [9] G. Landi, *Problems of position reconstruction in silicon microstrip detectors*, *Nucl.Instrum.Meth A* **554** (226) 2005
- [10] R. L. Golden, *Performance of a balloon-borne magnet spectrometer for cosmic ray studies*, *Nucl.Instrum.Meth A* **306** (366) 1991